

BBA 72222

## LOCATION AND DYNAMICS OF A MEMBRANE-BOUND FLUORESCENT HAPTEN

### A SPECTROSCOPIC STUDY

SUSAN G. STANTON, AARON B. KANTOR, ASHOT PETROSSIAN and JOHN C. OWICKI \*

*Department of Biophysics and Medical Physics, University of California, Berkeley, and Division of Biology and Medicine, Lawrence Berkeley Laboratory, University of California, Berkeley, CA 94720 (U.S.A.)*

(Received February 21st, 1984)

*Key words: Membrane-antibody interaction; Fluorescein-lipid hapten; Liposome; Lipid composition; Fluorophore orientation; Fluorescence*

In the preceding paper (Petrossian, A. and Owicki, J.C. (1984), *Biochim. Biophys. Acta* 776, 217–227), we describe the binding of a monoclonal anti-fluorescein antibody to a membrane bound fluorescein-lipid hapten. Those results suggest that some of the hapten fluorescein moiety is extended away from the membrane surface and is available for antibody binding, while some of the hapten is sequestered and not immediately available for antibody binding. In this paper, we carry out a spectroscopic study of the membrane-bound hapten and show that there is more than one physically distinct fluorophore environment, with the sequestered hapten associated with the phospholipid headgroup region. The amount of membrane-associated fluorophore depends upon the membrane lipid composition: most of the fluorophore is associated when the lipid is unsaturated or branched-chain phosphatidylcholines (PC), whereas the hapten is largely extended for PC/cholesterol mixtures. The effect of cholesterol on the availability of membrane-bound hapten to antibody binding is not unique to this system. The conversion between sequestered and extended hapten is slow (minutes).

### Introduction

In the preceding paper, we describe a fluorescent lipid hapten with the structure

fluorescein-chlorotriazinyl-triglycyl-DPPE (FG<sub>3</sub>P) [1]. There, we report the binding of monoclonal anti-fluorescein antibody to FG<sub>3</sub>P incorporated into phospholipid vesicles. Those studies were designed to determine the effects of membrane composition and antibody valency on the rate and strength of antibody-hapten binding. The FG<sub>3</sub>P fluorescence is effectively quenched by antibody binding, providing a sensitive method of monitoring the binding process.

If fully extended, the FG<sub>3</sub>P fluorescein-DPPE tether is 1.3 nm long. The antibody binding data for liposomes containing FG<sub>3</sub>P show that some of the hapten was extended away from the membrane surface, available for antibody binding, but suggest that some of the hapten was sequestered, and

\* To whom correspondence should be addressed.

#### Abbreviations:

5-DCTAF,	5-dichlorotriazinylaminofluorescein
DMPC,	dimyristoylphosphatidylcholine
DOPC,	dioleoylphosphatidylcholine
DPhPC,	diphytanoylphosphatidylcholine
	(di-3,7,11,15-tetramethylhexadecanoyl-PC)
DPPC,	dipalmitoylphosphatidylcholine
DPPE,	dipalmitoylphosphatidylethanolamine
FG <sub>3</sub> P,	fluorescein-chlorotriazinyl-triglycyl-DPPE
PC,	phosphatidylcholine
PE,	phosphatidylethanolamine
TLC,	thin-layer chromatography

not immediately available for antibody binding. The equilibrium between extended and sequestered antibody was highly dependent upon membrane lipid composition.

Investigators studying other systems have also come to the conclusion that their hapten was partly or completely sequestered in some membrane systems, but extended and available for antibody binding in others, particularly in the presence of cholesterol [2–4]. Our fluorescent hapten is an ideal system for the study of this phenomenon, since fluorescence spectroscopy is a proven method for studying fluorophore environment and dynamics [5–7]. We therefore have undertaken a spectroscopic study of our probe in a variety of phospholipid vesicles. We have measured the FG<sub>3</sub>P fluorescence spectrum as a function of lipid composition, pH, and probe concentration; we have determined the spectral polarization properties and measured fluorescence lifetimes. The questions we address include the following: Is the sequestered probe in the aqueous phase, but not sufficiently extended to allow antibody binding? Or is it located in the lipid headgroup region, or in the hydrocarbon interior? What factors affect the extended-sequestered equilibrium? How mobile is the probe? How fast is the extended-sequestered exchange?

## Materials and Methods

**Chemicals.** DMPC, DPPC, and DPhPC (diphytanoyl-PC) were obtained from Avanti Polar Lipids Inc. (Birmingham, AL), and were one spot on TLC. Egg PC was obtained from GIBCO Laboratories (Grand Island, NY). All other chemicals, unless otherwise noted, were obtained from Sigma Chemical Co. (St. Louis, MO), and were used without further purification. The detailed synthesis of FG<sub>3</sub>P will be reported elsewhere (Petrossian, Kantor and Owicki). The FG<sub>3</sub>P used previously [1] has 90% of the fluorescence running as one spot on TLC. For study of multiple fluorescent species, the FG<sub>3</sub>P was subjected to an additional preparative TLC step on silica gel developed with chloroform/methanol/water/acetic acid (65:25:4:2, v/v). This FG<sub>3</sub>P ran as one spot on TLC; its spectral properties were indistinguishable from those of the 90% pure form.

**Buffers.** Unless otherwise noted, experiments were performed in borate-buffered saline (BBS), with 50 mM boric acid adjusted to pH 9.5 with KOH and KCl added to give a final osmolarity of 310 mosM. At pH 9.5 the FG<sub>3</sub>P fluorescein moiety is almost entirely in its dianion \* form in DMPC, DPPC, and PC/cholesterol mixtures. The monoclonal anti-fluorescein antibody used in these studies [1] was stable at this pH. Borate, carbonate, and phosphate buffers, all 310 mosM, were used in the pK<sub>a</sub> determination studies.

**Vesicles.** Ethanol injection vesicles were made according to the procedure of Kremer et al. [8]. The appropriate mixture of lipid, FG<sub>3</sub>P, and ethanol was injected through a motor-driven Hamilton syringe into a stirred round-bottom flask containing 2 to 5 ml of buffer at 70 °C.

**Fluorescence measurements.** Fluorescence measurements were made on a Spex Fluorolog 2 fluorometer with both excitation and emission double monochrometers. The light source was a 450 watt xenon arc lamp. The fluorescence was detected with a Hamamatsu R928 phototube with photon counting. Typical excitation slits were 1 nm, emission slits 1 to 5 nm. Fluorescence spectral intensities were the ratio of excitation to reference intensities and were thus corrected for lamp spectral shape; emission spectra were corrected for wavelength-dependent monochromator throughput and detector sensitivity. Polarization measurements were made with uv Glan-Thompson polarizers in excitation and emission light paths. The parallel and perpendicular intensities,  $I_{||}$  and  $I_{\perp}$ , were corrected for instrumental artifacts in the standard way [9], and the polarization  $P$  was determined by the equation

$$P = \frac{I_{||} - I_{\perp}}{I_{||} + I_{\perp}} \quad (1)$$

The appropriate borate-buffered saline background was subtracted from each intensity measurement for vesicle preparations; the blank vesicle background was indistinguishable from the borate-buffered saline background. Trivial causes

\* Fluorophore dianion refers to the  $-2$  charge on the FG<sub>3</sub>P fluorescein moiety, for ease of comparison with sodium fluorescein. The FG<sub>3</sub>P molecule has an additional negative charge on the lipid phosphate group.

of depolarization such as fluorescence transfer and light scattering were minimized by using low lateral probe concentrations and solutions of low turbidity. At some sacrifice in signal-to-noise, each sample in the polarization study had an optical density below 0.01, hence the observed polarization was equal to the extrapolated polarization at zero optical density [10].

**$pK_a$  determination.** A fluorescent molecule with monoanion form  $m^-$  and dianion form  $d^{2-}$



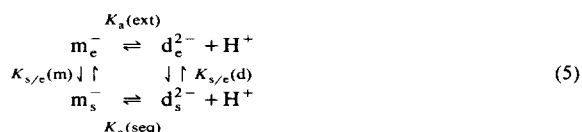
has an observed fluorescence intensity per mole  $I$  given by

$$I = f_m I_m + f_d I_d \quad (3)$$

where  $f_m$  and  $f_d$  are the fractions of monoanion and dianion respectively, and  $I_m$  and  $I_d$  are the monoanion and dianion molar fluorescence intensities. The  $pK_a$  for this reaction can be determined experimentally by measuring the fluorescence intensity as a function of pH and fitting the data to the equation

$$pK_a = \log \frac{I - I_d}{I_m - I} + pH \quad (4)$$

Our system is more accurately described by the equation



where  $e$  designates extended fluorophore and  $s$  designates sequestered fluorophore,  $K_a(\text{ext})$  and  $K_a(\text{seq})$  are the monoanion-dianion equilibrium constants for the extended and sequestered fluorophores, respectively, and  $K_{s/e}(m)$  and  $K_{s/e}(d)$  are the sequestered-extended exchange equilibrium constants for monoanion and dianion, respectively. The observed  $K_a$  is given by the equation

$$K_a = \frac{([d_e^{2-}] + [d_s^{2-}])[H^+]}{([m_e^-] + [m_s^-])} \quad (6)$$

which is related to the constants of Eqn. 5 by the

equation

$$K_a = \frac{K_a(\text{ext}) + K_{s/e}(m) K_a(\text{seq})}{1 + K_{s/e}(m)} \quad (7)$$

For our system  $K_a(\text{ext})$  is greater than  $K_a(\text{seq})$ , and in the limiting case of mostly extended fluorophore,  $K_{s/e}(m) \ll 1$ , and  $K_a = K_a(\text{ext})$ . Similar analysis shows that in the limiting case of mostly sequestered fluorophore,  $K_{s/e}(d) \gg 1$ , and  $K_a = K_a(\text{seq})$ .

The  $pK_a$  determined by fluorescence spectroscopy is a weighted average of ground and excited state  $pK_a$  values [11]. The ground state  $pK_a$  we measured for sodium fluorescein (6.6 by absorption spectroscopy) is slightly higher than the value determined by fluorescence (6.3). The fluorescence excitation spectrum as a function of pH for a fluorescein-like system described solely by Eqn. 2 will show an isosbestic point. This is also approximately true for a system described by Eqn. 5, if the spectral differences between sequestered and extended fluorophore are relatively small. The fluorescence data will not show an isosbestic point and the data cannot be fit to Eqn. 4 if Eqn. 2 or Eqn. 5 is not the only pH dependent reaction in the pH range of interest. The data will also not fit to Eqn. 4 if the local pH of the fluorophore is not equal to the bulk pH or to the bulk pH plus a constant.

**Partition experiments.** A solution of  $10^{-6}$  M dichlorotriazinylaminofluorescein (5-DCTAF, Research Organics, Cleveland, OH) in borate-buffered saline/hexane (1:1, v/v) was mixed vigorously. Partition of the fluorophore was determined by measuring the fluorescence in the borate-buffered saline phase and in the hexane phase made 0.1 M in  $NH_3$ .

**Lifetime measurements.** Fluorescence lifetime measurements were made at the Stanford Linear Accelerator lifetimes port. The experimental apparatus there has been described previously [12]. The light source was synchrotron radiation with a pulse width of 200 ps full width at half maximum. The entire system, including the radiation source and counting electronics, had 700 ps full width at half-maximum response. Decay curves were deconvoluted and fit to one or two exponentials with a non-linear least-squares fitting routine, Modelaide [13].

## Results and Discussion

### *Spectral identification of extended and sequestered hapten*

The excitation maximum (492 nm) of aqueous fluorescein dianion is independent of emission wavelength and vice versa, as is characteristic of a single fluorescent species. In pure PC membranes, the FG<sub>3</sub>P excitation maximum depends upon emission wavelength, as shown in Fig. 1. This presence of multiple spectroscopic species indicates more than one physical location for the FG<sub>3</sub>P fluorescein moiety. An alternative cause of multiple fluorescent species is incomplete solvent relaxation on the nanosecond time scale about a fluorophore in a single location. However, incomplete solvent relaxation cannot explain the correlation of red shift with hapten unavailability to antibody binding described below.

The fluorescence excitation and emission maxima for FG<sub>3</sub>P dianion are red-shifted from those of fluorescein dianion (see Fig. 2), with the amount of red shift dependent on the membrane lipid composition (see Table 1). The unsaturated and branched-chain PC have spectra with relatively large red-shifts, whereas the PC-cholesterol mixtures show very slight red-shifts. These general trends are mirrored in the antibody binding data: the unsaturated and branched-chain PC have a

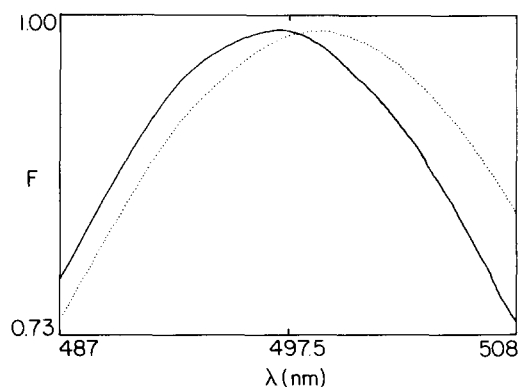


Fig. 1. FG<sub>3</sub>P excitation spectra as a function of emission wavelength. Excitation spectra of FG<sub>3</sub>P in DMPC vesicles, pH 9.5, 25°C. The left spectrum was taken with emission wavelength 515 nm, the right spectrum with emission wavelength 525 nm. *F* is the fluorescence intensity in arbitrary units; the two spectra have been normalized to the same peak intensity. The spectrum of blank vesicles cannot be distinguished from the baseline.

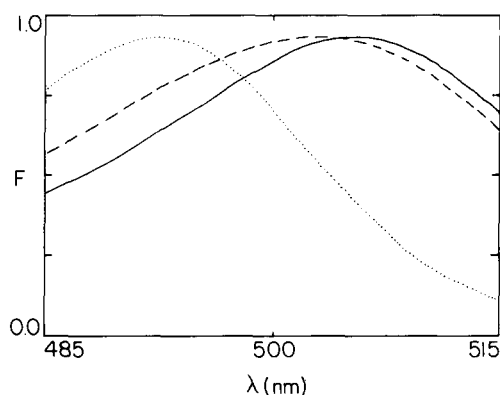


Fig. 2. Fluorescein and FG<sub>3</sub>P excitation spectra. Fluorescence excitation spectra of 10<sup>-7</sup> M fluorescein dianion (dots), 10<sup>-7</sup> M FG<sub>3</sub>P in DPPC (dashed), and 10<sup>-7</sup> M FG<sub>3</sub>P in DPhPC (solid) at 25°C. The emission wavelength was 525 nm. *F* is the fluorescence intensity in arbitrary units.

great deal of sequestered hapten, while the hapten in PC/cholesterol mixtures is mostly extended [1]. The correlation between spectral red-shift and unavailability for antibody binding is not perfect, however. The red-shift depends not only upon the relative hapten populations, but also on the red-shift of the sequestered hapten, which may be slightly lipid dependent. The antibody binding depends not only upon the relative populations of

TABLE I

FLUORESCENT SPECTRAL MAXIMA AND *pK<sub>a</sub>* VALUES

Solvent or lipid composition	Excitation maximum (nm)	Emission maximum (nm)	p <i>K</i> <sub>a</sub>
Fluorescein			
Borate-buffered saline	492	513	6.3
Methanol (0.1 M NH <sub>3</sub> )	498	519	
Ethanol (0.1 M NH <sub>3</sub> )	502	521	
FG <sub>3</sub> P			
Methanol (0.1 M NH <sub>3</sub> )	498	519	7.3
Ethanol (0.1 M NH <sub>3</sub> )	502	521	
FG <sub>3</sub> P incorporated into phospholipid vesicles			
DMPC/cholesterol (2 : 1)	495	518	8.4
DPPC/cholesterol (2 : 1)	497	520	
DMPC	499	522	
DPPC	504	524	8.4
Egg PC	503	524	
DOPC	504	524	
DPhPC	506	527	

extended and sequestered hapten, but also upon the population exchange rate and the amount of exterior lipid in the vesicle preparation. DMPC shows an intermediate red-shift and an anomalously high extent of antibody binding, due to fast conversion between the available and unavailable hapten plus hapten flip-flop, as described below. We conclude that the extended probe has an excitation spectrum with little or no shift from that of fluorescein dianion, whereas the sequestered probe has distinctly red-shifted excitation and emission spectra. This conclusion is further supported by the polarization data presented below.

The sequestered hapten must be physically protected from antibody binding, and one can hypothesize several means by which this might be accomplished. The hapten could be aggregated, protecting individual fluorophores from antibody binding. The fluorescein-DPPE tether could be bent with the fluorophore pointed back towards the membrane surface while still residing in the aqueous phase. The fluorophore could actually be associated with the membrane, either in the hydrocarbon or headgroup region. We shall examine these possibilities below.

*The sequestered hapten is not in the aqueous phase*

The fluorophore monoanion-dianion  $pK_a$  values for  $FG_3P$  depend on membrane lipid composition (see Table I and Fig. 3), and are all higher than the value of 6.3 measured for sodium fluorescein in water. The  $pK_a$  shifts may be caused by a difference between local and bulk pH, or by the fluorophore residing in an environment with a lower dielectric constant than that of water.

Gouy-Chapman theory predicts the pH near a membrane surface for a given surface charge, bulk pH, and solution ionic composition [14]. For our neutral membranes and high-ionic-strength buffers, no  $pK_a$  shift is predicted for fluorophore in the aqueous phase. According to this theory, the addition of charged lipid to the bilayer shifts the apparent  $pK_a$  (measured vs. bulk pH), especially in low-ionic-strength buffers. In qualitative agreement with this prediction, the apparent  $pK_a$  of  $FG_3P$  in DMPC vesicles dropped from 8.4 to approx. 7.9 when 5% hexadecyltrimethylammonium cation was incorporated into the membrane in low-ionic-strength buffers (10 mM). Even

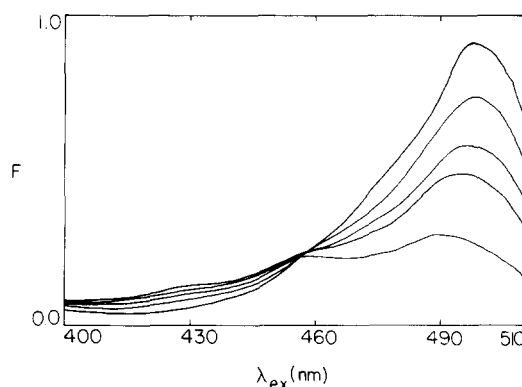


Fig. 3. Excitation spectra of  $FG_3P$  in DMPC as a function of pH. From top to bottom (at 500 nm) the spectra are for the pH values 10.35, 8.91, 8.51, 8.29, and 7.77 at 18 °C. The isosbestic point at 458 nm is seen except for the pH 7.77 spectrum; this pH shows the first sign of the neutral species. The fluorescent intensity  $F$  is in arbitrary units; the emission wavelength was 560 nm. Similar results are obtained at 25 °C.

under these drastic conditions the  $pK_a$  shift was small compared to the original difference between the  $pK_a$  values of sodium fluorescein (6.3) and  $FG_3P$  in DMPC (8.4). Thus a difference between bulk and local pH for fluorophore in the aqueous phase cannot explain the observed  $pK_a$  shifts.

The  $pK_a$  shifts are due to the fluorophore residing in a region of lower dielectric constant, either at the membrane surface or inside the membrane. Similar  $pK_a$  shifts have been observed by Fromherz et al. for a series of dye molecules located at membrane and micelle surfaces: dyes that increase their charge with increasing pH have higher  $pK_a$  values in neutral membranes and micelles than as free dyes in solution. These investigators attribute this effect to the lower dielectric constant of the membrane or micelle surface [15–17].

Cholesterol has a marked effect upon the probe pH behavior. The  $pK_a$  shift for DPPC/cholesterol (2:1) is much less than the shifts for DMPC and DPPC. The extended probe predominates in the presence of cholesterol, and the measured  $pK_a$  is weighted towards the  $pK_a$  for the extended monoanion-dianion transition (see Eqn. 7). For DMPC and DPPC more of the hapten is sequestered, and the measured  $pK_a$  is weighted more towards the  $pK_a$  for the sequestered fluorophore. The DMPC and DPPC pH dependent spectra show isosbestic points, while the DPPC/cholesterol (2:1) spectra

has no isosbestic point and shows little spectral evidence of monoanion as the dianion disappears. For this reason, the data do not fit exactly to Eqn. 4 and  $pK_a$  determined is approximate. This behavior suggests that the neutral-monoanion transition occurs at a pH only slightly below that of the monoanion-dianion transition in this system.

*The sequestered hapten is associated with the membrane headgroup region*

5-DCTAF dianion, a water-soluble form of our hapten, was found to have an unmeasurably low partition coefficient from borate-buffered saline into hexane, with an upper limit of  $10^{-4}$ . This result is not particularly surprising, in view of the  $-2$  fluorophore charge. Given that the sequestered hapten is not in the aqueous phase and not in the membrane hydrocarbon region, we conclude that the fluorophore is associated with the membrane headgroup region. We use the term 'headgroup region' to include the glycerol backbone and polar headgroup regions, making no attempt to differentiate between the two.

*The hapten does not aggregate at low lateral concentrations*

Lateral hapten aggregation is likely to lead to fluorescence quenching and a non-linear fluorescence intensity response to antibody binding. We therefore studied the (lateral) concentration quenching of  $FG_3P$  in fluid DMPC vesicles (see Fig. 4). At a probe concentration of 1.6 mol%, 50%

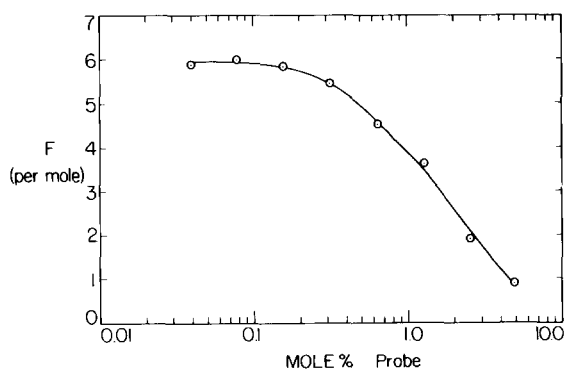


Fig. 4. Concentration quenching. The fluorescence intensity  $F$  (in arbitrary units) at  $25^\circ\text{C}$  is shown per mole of  $FG_3P$  in DMPC vesicles vs. probe mol% of total lipid. The total lipid concentration was  $55\ \mu\text{M}$  for probe concentrations 0.04% to 0.6%,  $7\ \mu\text{M}$  for probe concentrations 0.6% to 5%.

quenching was observed. It appears that at high probe concentrations, aggregates formed that have low quantum yields. This has been reported for sodium fluorescein [18].

Quenching is usually enhanced by Förster energy transfer. Transfer among the monomeric probes does not itself cause quenching, but transfer to an aggregate does. Hence, monomers act as radiation collecting antennae with aggregates as traps [19]. For fluorescein dianion, energy transfer is calculated to be 50% efficient for two molecules separated by a distance  $R_0$  of 5.0 nm. At 1.6 mol% probe one can then calculate [20] an overall transfer efficiency of at least 85%. Thus, energy transfer must contribute to our observed quenching and fewer than half of the probe molecules are aggregated at 1.6 mol%, assuming the aggregate quantum yield is low. Further quantitative experiments are beyond the scope of this work. To obtain fluorescence intensities linear in the number of probe molecules per vesicle and to avoid quenching complications, the experiments described in this paper and the one preceding [1] were carried out at low lateral concentrations ( $\leq 0.1$  mol%) except where noted.

*Lifetimes*

Fluorescein dianion has a lifetime of 4.0 ns in aqueous solution [21]. We measured a lifetime of  $3.9 \pm 0.1$  ns for  $FG_3P$  in DMPC membranes (see Fig. 5). The data fit well to a single exponential,

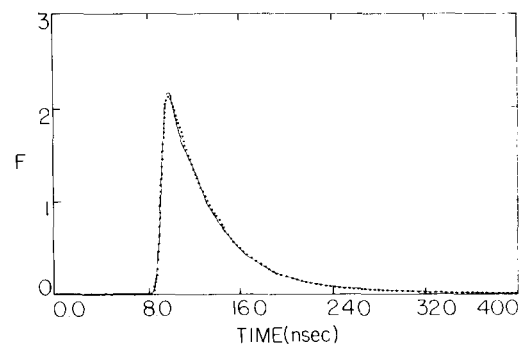


Fig. 5. Fluorescence lifetime. The fluorescence intensity  $F$  in arbitrary units at  $33^\circ\text{C}$  is shown as a function of time. The dots are data points; the smooth curve is the first of a single 3.9 ns decay convoluted with the instrumental line shape. The lipid was  $1.3 \cdot 10^{-3}$  M DMPC with  $3.9 \cdot 10^{-6}$  M  $FG_3P$  (0.3%). The excitation wavelength was 480 nm, the emission wavelength 500–550 nm.

and no significant improvement in the fit was obtained by attempting to fit the data to two exponentials. It is apparent that the fluorescence lifetime is not very sensitive to changes in the fluorophore environment. This is not surprising, since the fluorescence lifetime changes only slightly from water to various alcohols [22]. Since the  $\text{FG}_3\text{P}$  lifetime is very close to that of aqueous fluorescein, the quantum yield of  $\text{FG}_3\text{P}$  in the membrane environment is close to the 93% value measured for fluorescein dianion [21].

### Hapten mobility

Steady-state fluorescence polarization measures the rotational mobility of a fluorescent molecule on the nanosecond time scale. Depolarization occurs either when the excitation and emission transition dipoles are not parallel, or when the fluorophore rotates during the fluorescence lifetime. The intrinsic polarization  $P_0$  of the fluorescein dianion has been measured [23,24]. For the long-wavelength region of the excitation spectrum (460–530 nm), the polarization has a value  $P_0 = 0.492 \pm 0.005$  [24]. This value is close to the limiting value of 0.5 for parallel excitation and emission transition dipoles, indicating that depolarization of fluorescein fluorescence is due solely to fluorophore rotation.

The polarization excitation spectra of  $\text{FG}_3\text{P}$  dianion in solutions of low and high viscosity are shown in Fig. 6 (curves a and b). The long-wavelength polarization value in glycerol,  $P = 0.48 \pm 0.01$ , agrees well with the fluorescein  $P_0$ . Curves c through e show the polarization spectra of  $\text{FG}_3\text{P}$  in vesicles of various lipid compositions. As expected, the probe fluorophore shows a mobility intermediate between free rotation and complete immobilization, with the exact value of  $P$  dependent upon membrane lipid composition.

Both the DPPC and DPPC/cholesterol (2:1) spectra show two components. The long-wavelength component (510–530 nm) has a polarization weighted towards the polarization of the fluorophore with the red-shifted excitation spectrum, and is more polarized (less mobile) than the short-wavelength component (450–480 nm), which is weighted towards the polarization of the unshifted fluorophore. This evidence supports our earlier conclusion that probe with a red-shifted

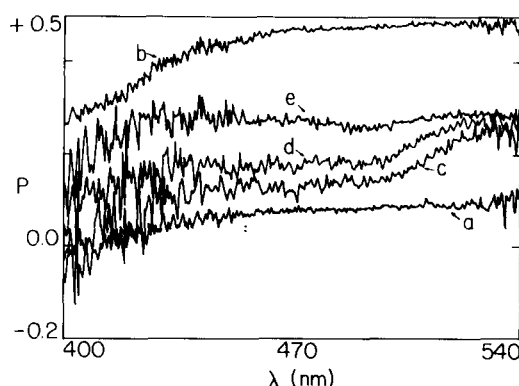


Fig. 6. Polarization excitation spectra. Curve a:  $3.2 \cdot 10^{-7}$  M  $\text{FG}_3\text{P}$  in ethanol, 0.1 M  $\text{NH}_3$ , 20 °C. Curve b:  $3.2 \cdot 10^{-7}$  M  $\text{FG}_3\text{P}$  in 5% (v/v) ethanol, 95% glycerol, 0.1 M  $\text{NH}_3$ , 2 °C. Excitation and emission slits for curves a and b were 1.8 nm and 4.9 nm, respectively. Curves c–e:  $1.4 \cdot 10^{-8}$  M  $\text{FG}_3\text{P}$  incorporated into phospholipid vesicles of (c) DPPC/cholesterol (2:1), (d) DPPC, and (e) DPhPC. Total lipid was  $3.6 \cdot 10^{-5}$  M, temperature 25 °C, excitation slits 1.8 nm and emission slits 10.8 nm. Blank vesicles without probe showed no scattering at excitation wavelengths below 540 nm. In all cases the emission wavelength was 560 nm.

excitation maximum is membrane associated, whereas probe with an unshifted excitation maximum is extended. The DPhPC spectrum is more polarized than the DPPC and DPPC/cholesterol (2:1) spectra, and is essentially flat from 450 to 530 nm. Thus, one relatively rotationally immobilized species is the major component in these vesicles. The polarization progression ethanol solution < DPPC/cholesterol < DPPC < DPhPC < glycerol solution is in complete agreement with the red-shift and antibody binding results for these preparations.

### Dynamics

A great deal about the exchange dynamics between the sequestered and extended probe can be deduced from the antibody binding results. If the exchange between the sequestered and extended forms were very fast, antibody binding to all hapten on the vesicle outer surface would be pseudo first order in the presence of excess antibody. Instead, a reasonably fast initial antibody binding was followed by a slower binding process, with rates dependent upon lipid composition [1]. Thus we can conclude that interchange between the ex-

tended and sequestered forms is a slow (minutes) process.

DMPC has proved to be a special case. At or above the phase transition temperature, and at pH 9.5, where the fluorophore is almost completely in its dianion form, we observed up to 87% quenching of the probe upon antibody binding. This means more than 87% of the haptens were bound, since there was some residual fluorescence from bound haptens (3% for sodium fluorescein [25], somewhat more for FG<sub>3</sub>P [1]). Since only about 60% of the lipid molecules were in the outer monolayer of these small unilamellar vesicles, it is clear that FG<sub>3</sub>P from the vesicle interior was bound by antibodies. The 150 kDa antibody was too large to leak into the vesicle; thus we must conclude that the FG<sub>3</sub>P flip-flopped across the DMPC bilayer despite the  $-3$  charge on the headgroup. The flip-flop mechanism may well involve conversion of the fluorophore to its neutral state or pairing with counter ions. The observed flip-flop was relatively fast, since the antibody binding was complete in minutes. Flip-flop of our probe was not observed in any other lipid system we studied, including DPPC below, at, and above its phase transition temperature. DMPC is one of the shortest PC to form stable bilayers, and other investigators have observed unusually high ionic permeability for DMPC model membranes (Hubbell, W.L., personal communication).

## Conclusions

In conclusion, we find that the fluorescein moiety of FG<sub>3</sub>P incorporated into model membranes exists in two states: associated with the membrane headgroup region, and extended out away from the membrane surface. We note that while it has been conceptually useful to treat the hapten as existing in two distinct locations, the data are equally consistent with a continuum of hapten locations between the fully extended and fully associated positions. The extended probe has an excitation spectrum similar to fluorescein and an intermediate polarization; the sequestered probe has a red-shifted spectrum and a somewhat higher polarization. The relative amounts of sequestered and extended hapten are quite sensitive to the composition of the phospholipid vesicles. For ex-

ample, the nature of the acyl chain is important in PC vesicles: there was more extended probe for saturated chains than for unsaturated or branched chains in our studies. However, this was not related in any simple way to membrane 'fluidity'.

The large increase in extended probe population upon the addition of cholesterol is particularly interesting, since similar increases in availability for antibody binding have been observed with vesicles bearing other haptens: nitroxide [2], dinitrophenyl [3], and dansyl [4]. Cholesterol reduces the partition of all three of these haptens (in water-soluble form) into phosphatidylcholine membranes [3,26,27]. The four haptens, including fluorescein, vary in size from about 150 to 350 daltons and in charge from neutral to  $-2$  under the experimental conditions. All are cyclic molecules of moderate hydrophilicity, and the similarity of their behavior could be related to this factor.

One observation suggesting more general applicability concerns the ability of liposomes to fix (activate) serum complement when they contain cardiolipin as an antigen. Cardiolipin is structurally unlike any of the haptens mentioned above, yet the inclusion of cholesterol in the liposomes strongly increases polyclonal antibody-dependent complement fixation [28]. It seems likely that enhanced antibody binding to cholesterol-containing membranes caused the increased immunological reactivity.

An explanation of the phenomenon in molecular terms is difficult at this time. Since it operates both above and below the phase transition temperature of the phospholipid, it is unlikely to be related fundamentally to the acyl chain order or dynamics. Cholesterol has opposite effects on these properties in the two temperature ranges. Links to the phospholipid headgroup dynamics are likewise tenuous, since there is evidence that cholesterol again has opposite effects above and below the phase transition [29]. One effect of cholesterol at all temperatures is to decrease the lateral density of head groups. NMR clearly shows a disruption of intermolecular interactions between head groups when cholesterol is added to DOPC bilayers [30]. Such changes could plausibly alter the degree of probe-membrane association. The magnitude and direction of the effect are not, however, obvious *a priori*. Another indication of effects of cholesterol



on the headgroup and ester regions is an increase in the membrane dipole potential by cholesterol in glycerolmonooleate bilayers [31]. This would destabilize negatively charged molecules that bind close to the membrane but outside the dipolar layer, a likely placement for the sequestered probe.

### Acknowledgements

We thank the staff of the Stanford Synchrotron Radiation Laboratory for access to their lifetimes port. S.G.S. is a N.I.H. postdoctoral fellow. A.B.K. is a N.I.H. trainee. A.P. is a Neshan Zovick fellow. This work was supported by the following grants: N.I.H. R01-AI-19605-02, U.C. Cancer Res. Coord.Comm. Grant 80B2, and B.R.S.G. grant 2-S07-RR-7006 from the Biomedical Research Support Program, N.I.H.

### References

- Petrossian, A. and Owicki, J.C. (1984) *Biochim. Biophys. Acta* 776, 217–227
- Brûlet, P. and McConnell, H.M. (1977) *Biochemistry* 16, 1209–1217
- Balakrishnan, K., Mehdi, S.Q. and McConnell, H.M. (1982) *J. Biol. Chem.* 257, 6434–6439
- Luedtke, R. and Karush, F. (1982) *Biochemistry* 21, 5738–5744
- Waggoner, A.S. and Stryer, L. (1970) *Proc. Natl. Acad. Sci. USA* 67, 579–589
- Azzi, A. (1975) *Rev. Biophys.* 8, 237–316
- Badley, R.A. (1976) in *Modern Fluorescence Spectroscopy* (Wehry, E.L., ed.), pp. 91–168, Plenum Publishing Co., New York
- Kremer, J.M.H., Van de Esker, M.W.J., Pathmamanoharan, C. and Wiersema, P.H. (1977) *Biochemistry* 16, 3932–3935
- Lakowicz, J.R. (1983) *Principles of Fluorescence Spectroscopy*, p. 126, Plenum Press, New York
- Lentz, B.R., Moore, D.M. and Barrow, D.A. (1979) *Biophys. J.* 25, 489–494
- Schulman, S.G. (1976) in *Modern Fluorescence Spectroscopy* (Wehry, E.L., ed.), Vol. 2, pp. 239–275, Plenum Press, New York
- Bucks, R.R. (1982) Ph.D. Thesis, p. 123, Stanford University
- Shrager, R.I. (1970) in Tech. Report No. 5, U.S. Department of Health, Education and Welfare
- McLaughlin, S. (1977) *Curr. Topics Membranes Transport* 9, 71–144
- Fernandez, M. and Fromherz, P. (1977) *J. Phys. Chem.* 81, 1755–1761
- Fromherz, P. and Masters, B. (1974) *Biochim. Biophys. Acta* 356, 270–275
- Fromherz, P. (1973) *Biochim. Biophys. Acta* 323, 326–334
- Pant, D.D. and Pant, H.C. (1968) *Indian J. Pure Appl. Phys.* 6, 238–243
- Lutz, D.R., Nelson, K.A., Gochanour, C.R. and Fayer, M.D. (1981) *Chem. Phys.* 58, 325–334
- Wolber, P.K. and Hudson, B.S. (1979) *Biophys. J.* 28, 197–210
- Weber, G. and Teale, F.W.J. (1958) *Trans. Faraday Soc.* 54, 640–647
- Schmillen, A. and Legler, R. (1967) in *Luminescence of Organic Substances*, Vol. 3 of Landolt-Bornstein, New Series (Hellwege, K.H. and Hellwege, A.M., eds.), Springer Verlag, New York
- Chen, R.F. and Bowman, R.L. (1965) *Science* 147, 729–732
- Szalay, L., Gati, L. and Sarkany, B. (1962) *Acta Phys. Hung.* 14, 217–223
- Kranz, D.M., Herron, J.N. and Voss, E.W., Jr. (1982) *J. Biol. Chem.* 257, 6987–6995
- Recktenwald, D.J. and McConnell, H.M. (1981) *Biochemistry* 20, 4505–4510
- Humphries, G.M.K. and Lovejoy, J.P. (1983) *Biophys. J.* 42, 307–310
- Humphries, G.M.K. and McConnell, H.M. (1975) *Proc. Natl. Acad. Sci. USA* 72, 2483–2487
- Shepherd, J.C.W. and Buldt, G. (1979) *Biochim. Biophys. Acta* 558, 41–47
- Yeagle, P.L., Hutton, W.C., Huang, C.-h. and Martin, R.B. (1977) *Biochemistry* 16, 4344–4349
- Szabo, G. (1974) *Nature* 252, 47–49